Supporting Information

Structural Evolution of Amorphous Precursors towards Crystalline Zeolites Visualized by *in-situ* X-ray Pair Distribution Function Approach

*Hiroki Yamada[1, 2], Satoshi Tominaka[2, 3], Koji Ohara[2], Zhendong Liu[1], Tatsuya Okubo[1] and Toru Wakihara[1]**

1) Department of Chemical System Engineering, The University of Tokyo, 7-3-1 Hongo, Bunkyo-ku, Tokyo 113-8656, Japan

2) JASRI, Kouto 1-1-1, Sayo-cho, Sayo-gun, Hyogo 679-5198, Japan

3) International Center for Materials Nanoarchitectonics (WPI-MANA), National Institute for Materials Science (NIMS), 1-1 Namiki Tsukuba, Ibaraki 305-0044, Japan.

Corresponding Author

Toru Wakihara
Associate Professor, Department of Chemical System Engineering
The University of Tokyo
7-3-1 Hongo, Bunkyo-ku, Tokyo 113-8656, Japan
Tel: +81-3-5841-7368 Fax: +81-3-5800-3806
Email: wakihara@chemsys.t.u-tokyo.ac.jp

Supplementary Figures

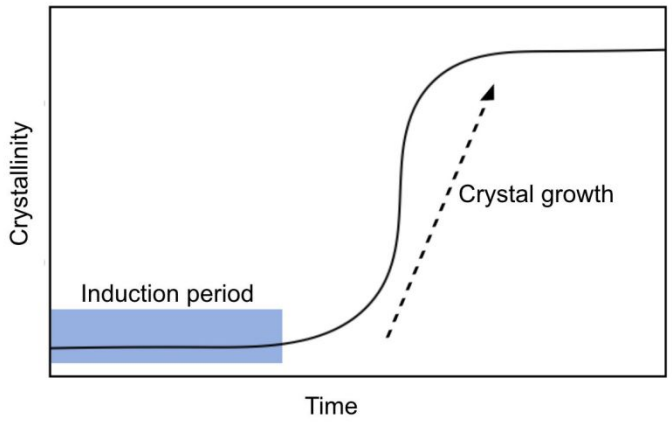

Figure S1 | Scheme representing the induction period of the synthesis of zeolite. An induction period (usually several hours ~ days) is needed before the nucleation of zeolites. After nucleation, rapid crystal growth occurs.

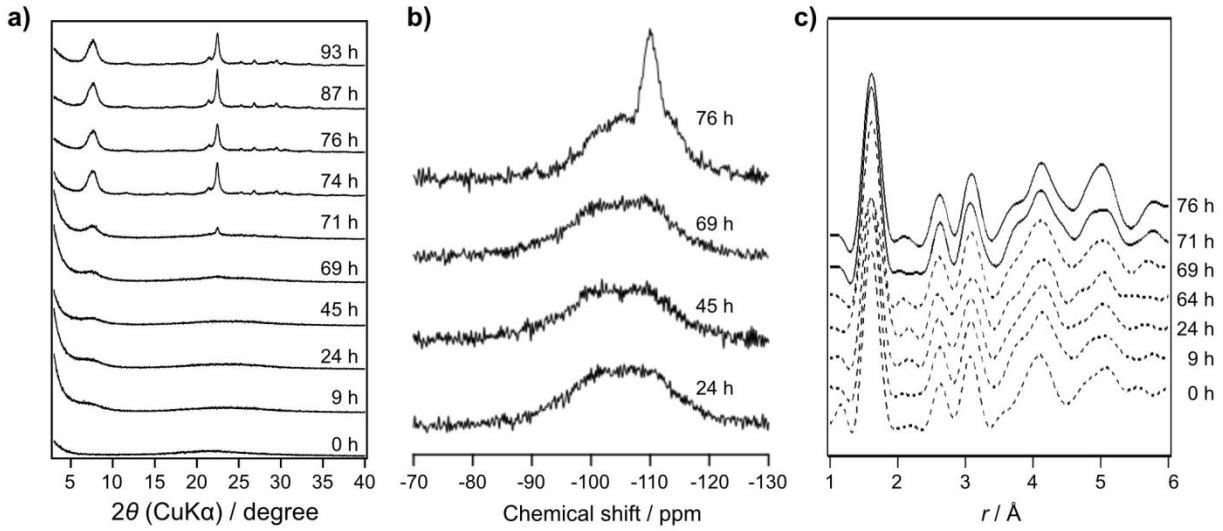

Figure S2 | Typical *ex-situ* XRD, ^{29}Si Magic Angle Spinning NMR spectra and X-ray PDF profiles of *BEA zeolites. (a) XRD patterns; (b) ^{29}Si NMR spectra; (c) $G(r)$ of the solid products. *BEA zeolites were synthesized as follows[1]. The starting mixture was prepared with a molar composition of 1.0 SiO_2 : 0.025 Al_2O_3 : 0.40 TEAOH (tetraethylammonium hydroxide) : 16 H_2O. Aqueous solutions of TEAOH (35 wt%, Sigma-Aldrich, USA) were used. Aluminum hydroxide (Wako Pure Chemical Industries, Japan) was dissolved in an aqueous solution of the organic structure-directing agent (OSDA) by heating the mixture overnight at 80°C. After dissolution, the solution was cooled to room temperature, and the required amounts of water and fumed silica (Cab-O-Sil M5, Cabot, USA) were added. Fumed silica was slowly added under stirring for 15 min at room temperature. Afterwards, all the reactants were poured into the autoclave and sealed, and, then, heated at 150°C under static conditions in an oven. After the hydrothermal treatment period, cold water was used to quench the autoclave. The solid product was repeatedly centrifuged and washed with deionized water until the aqueous mixture showed an approximately neutral pH. The recovered solid product was dried overnight at 80°C. After correcting the solid products, PDF measurements were conducted as described in Methods section. From Figure S2a, nucleation of the zeolites was confirmed after 71 h of synthesis. Figure S2b shows the ^{29}Si MAS NMR spectra are shown in. In the first stage of the synthesis, no difference was observed during the induction period (24–69 h). When the nucleation of the zeolite occurred, significant changes were observed (76 h). According to the PDF patterns during the induction period (Figure S2c), no obvious structural differences can be detected, but after the nucleation of the BEA zeolite, some structural changes can be detected. Therefore, *ex-situ* PDF analysis can be used to analyze the crystal growth step of the zeolite, but does not provide useful information of the structural changes during the induction period.

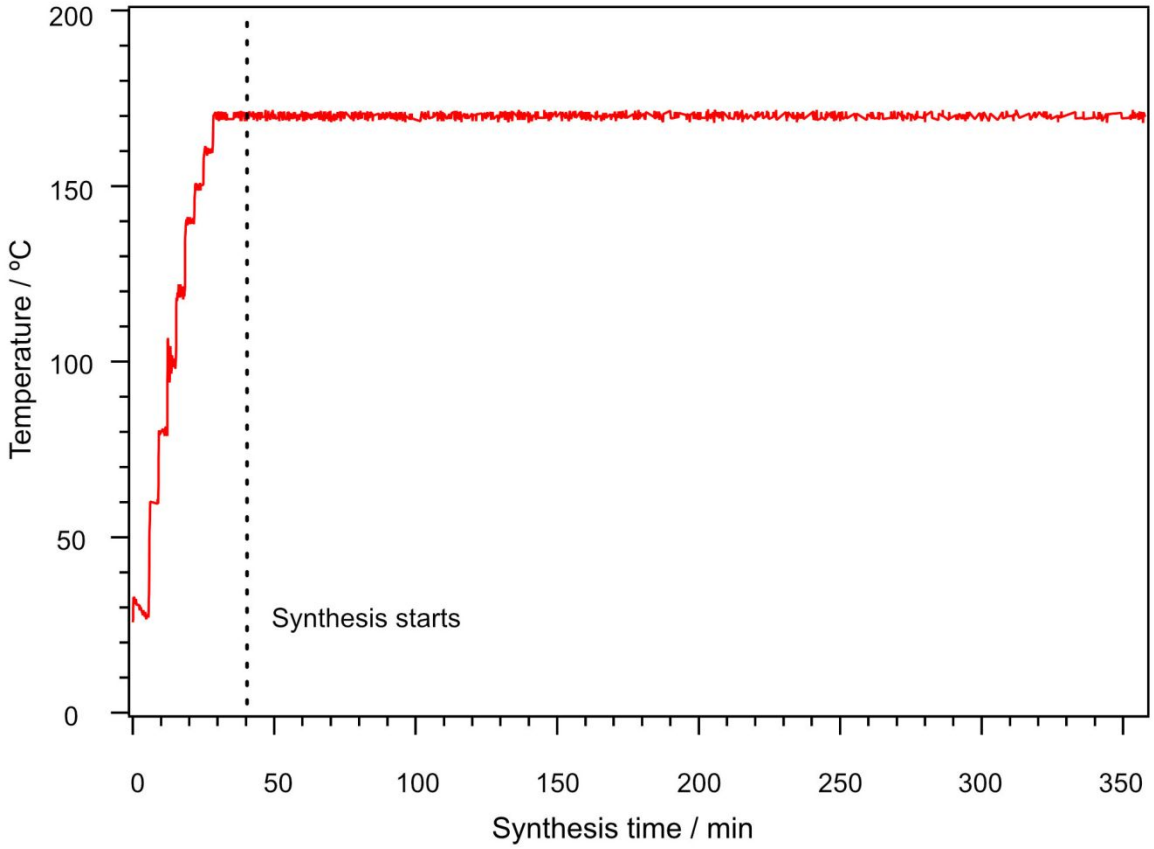

Figure S3 | Temperature profile for the synthesis of MFI: First, the solution was stirred for 5 min at room temperature, then the temperature increased by 10°C every 3 min. After the temperature reached 170°C, it was maintained until the crystallization finished. The beginning of the synthesis was set at 40 min to calculate the profiles of *in situ* XRDs, total PDFs and relative PDFs.

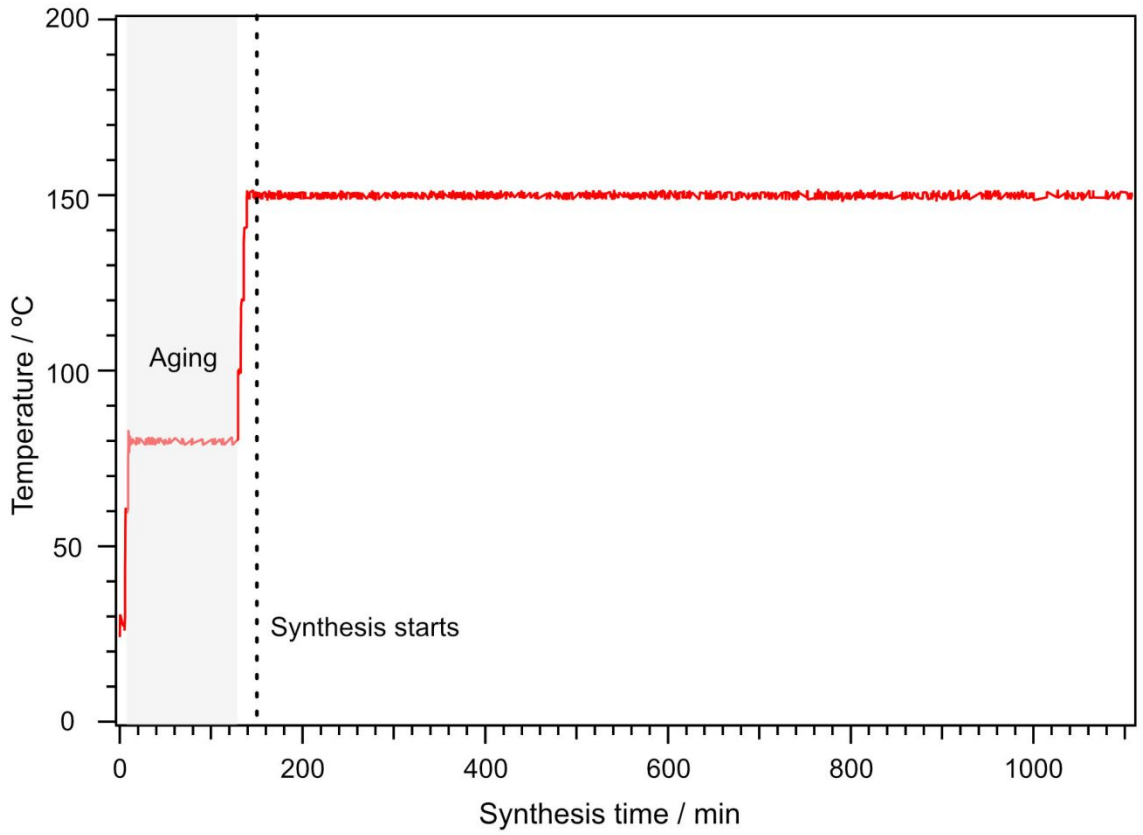

Figure S4 | Temperature profile for the synthesis of *BEA: First, the solution was stirred for 5 min at room temperature, then the temperature increased by 10°C every 3 min. After the temperature reached 80°C, the aging treatment was performed for 2 h. Then, the reactants were heated at 150°C at the same heating rate. The beginning of the synthesis was set at 150 min to calculate the profiles of *in situ* XRDs, total PDFs and relative PDFs.

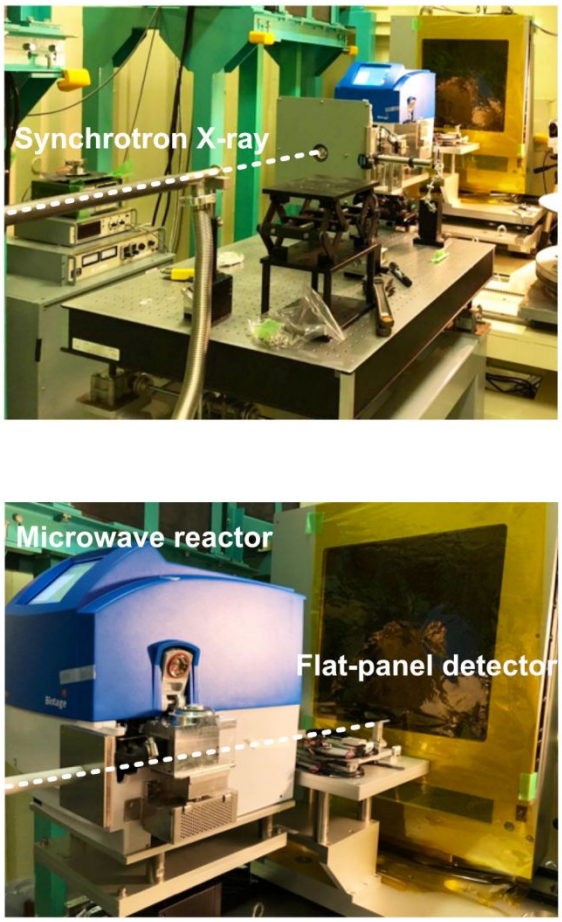

Figure S5 | Photographs of the experimental setting for *in situ* X-ray PDF measurements at BL08W in SPring-8: Synchrotron X-ray emission penetrated the vials fixed in the microwave reactor, and the scattering patterns were recorded by the flat panel detector every 1 min.

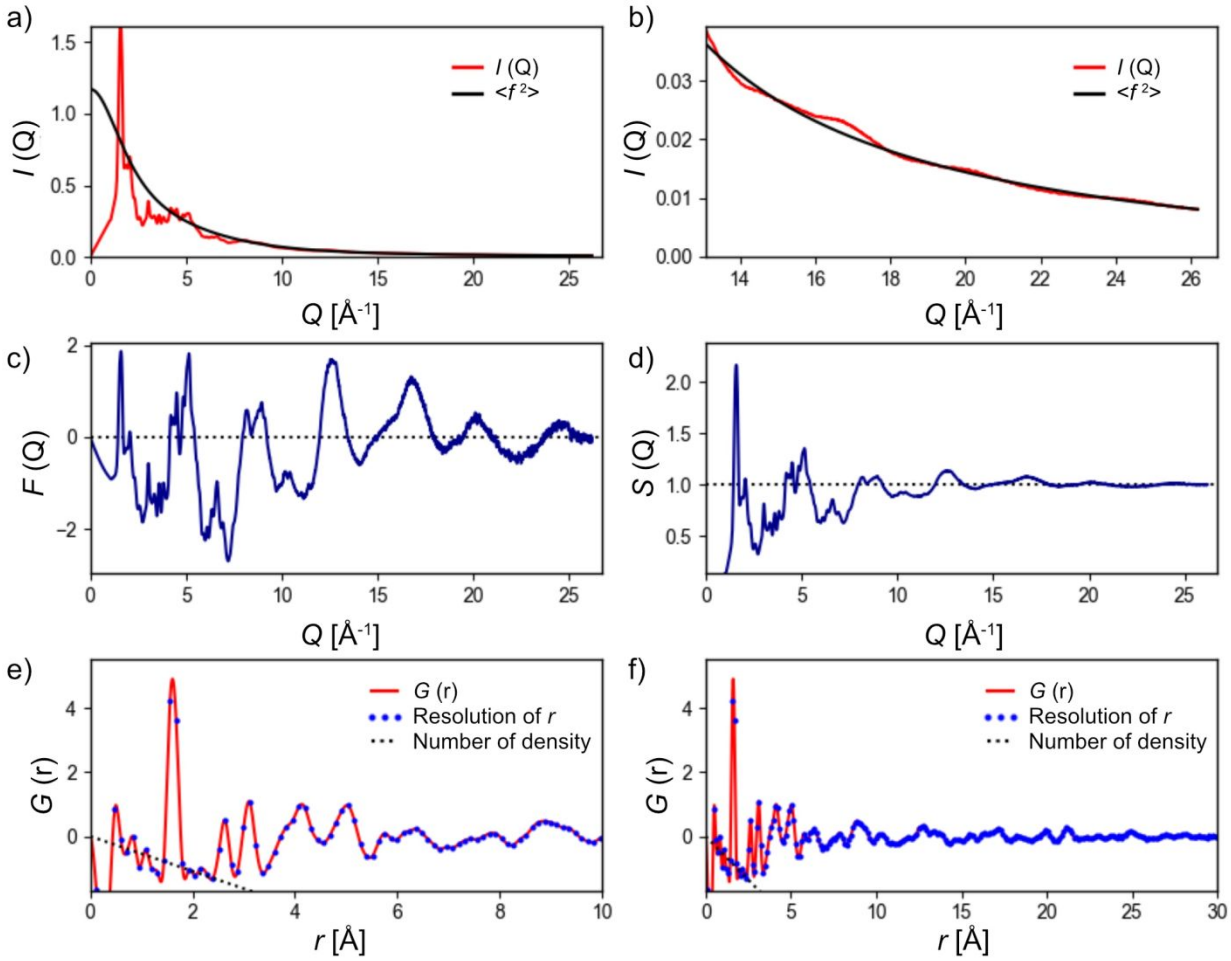

Figure S6 | Series of data used to calculate the X-ray PDF profiles of the MFI zeolite: a) elastic scattering pattern (a) full range and (b) magnification at the high Q range; (c) F (Q) ([S (Q)−1] * Q); (d) S (Q); (e) G (r) (magnification at the short r range); f) G (r) (full range). Blue dots in (e) and (f) indicate the resolution of r determined by π / Q_{Max}.

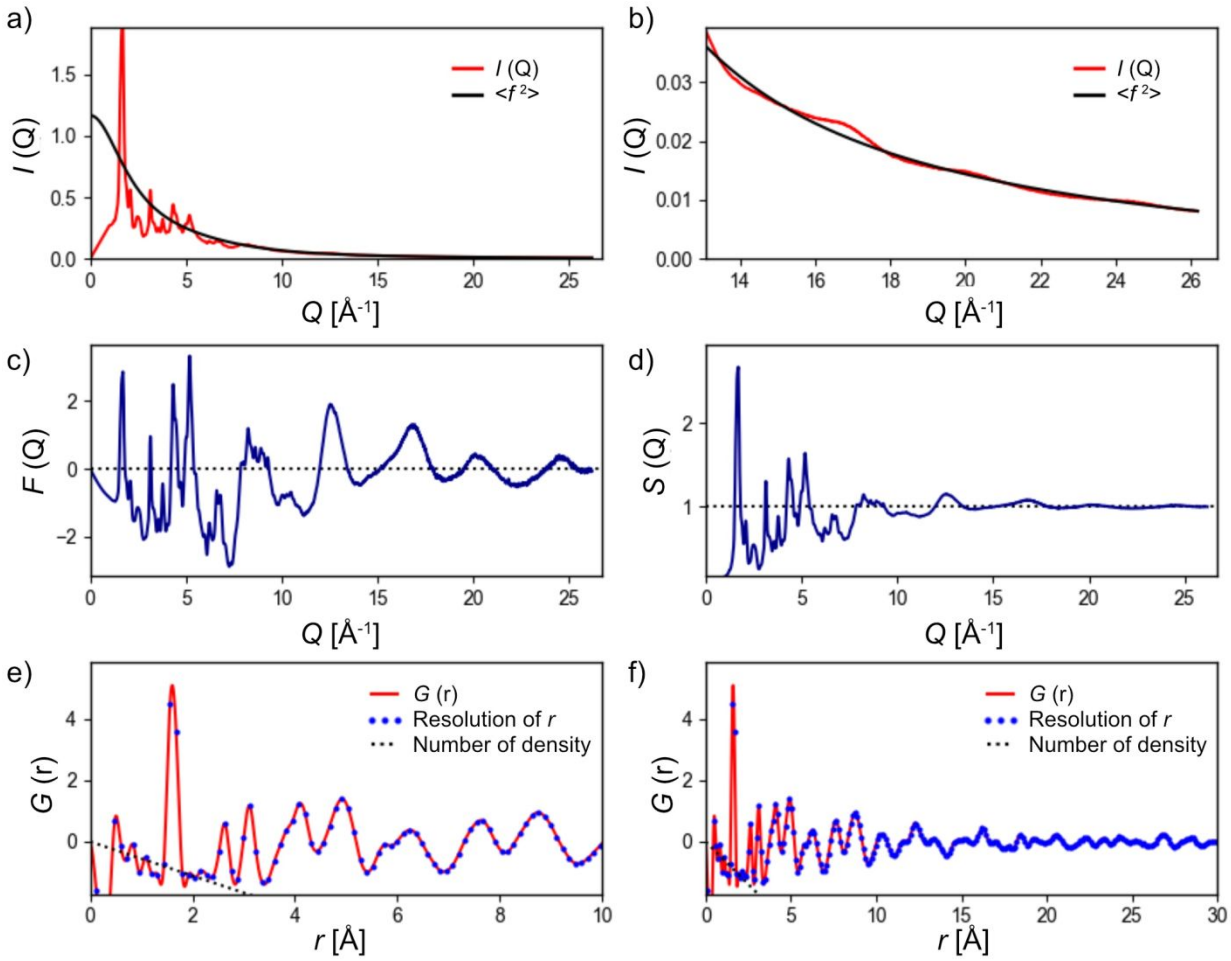

Figure S7 | Series of data used to calculate the X-ray PDF profiles of the *BEA zeolite: elastic scattering pattern (a) full range and (b) magnification at the high Q range; (c) F (Q) ([S (Q)−1] * Q); (d) S (Q); (e) G (r) (magnification at the short r range); (f) G (r) (full range). Blue dots in (e) and (f) indicate the resolution of r determined by π / Q_{Max}.

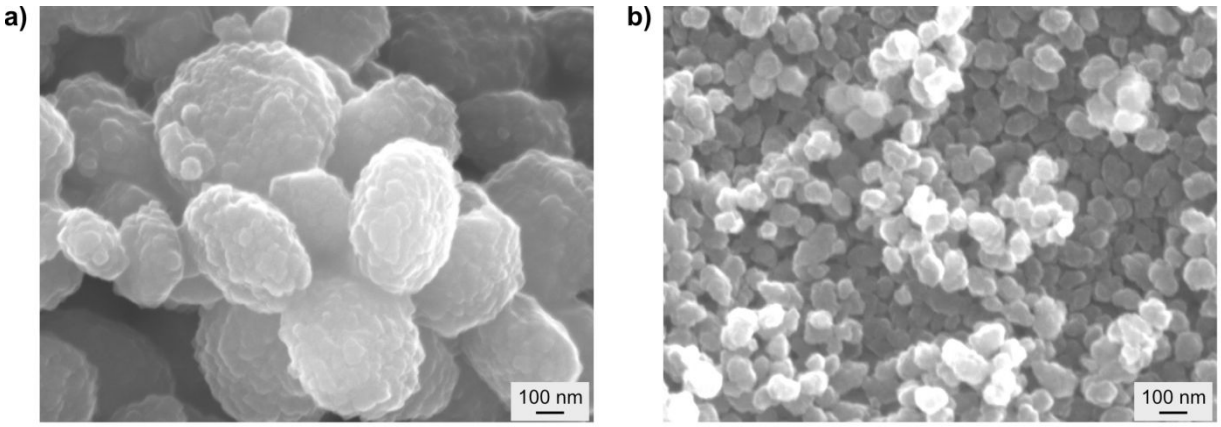

Figure S8 | SEM images of the MFI and *BEA zeolites. (a) MFI and (b) *BEA.

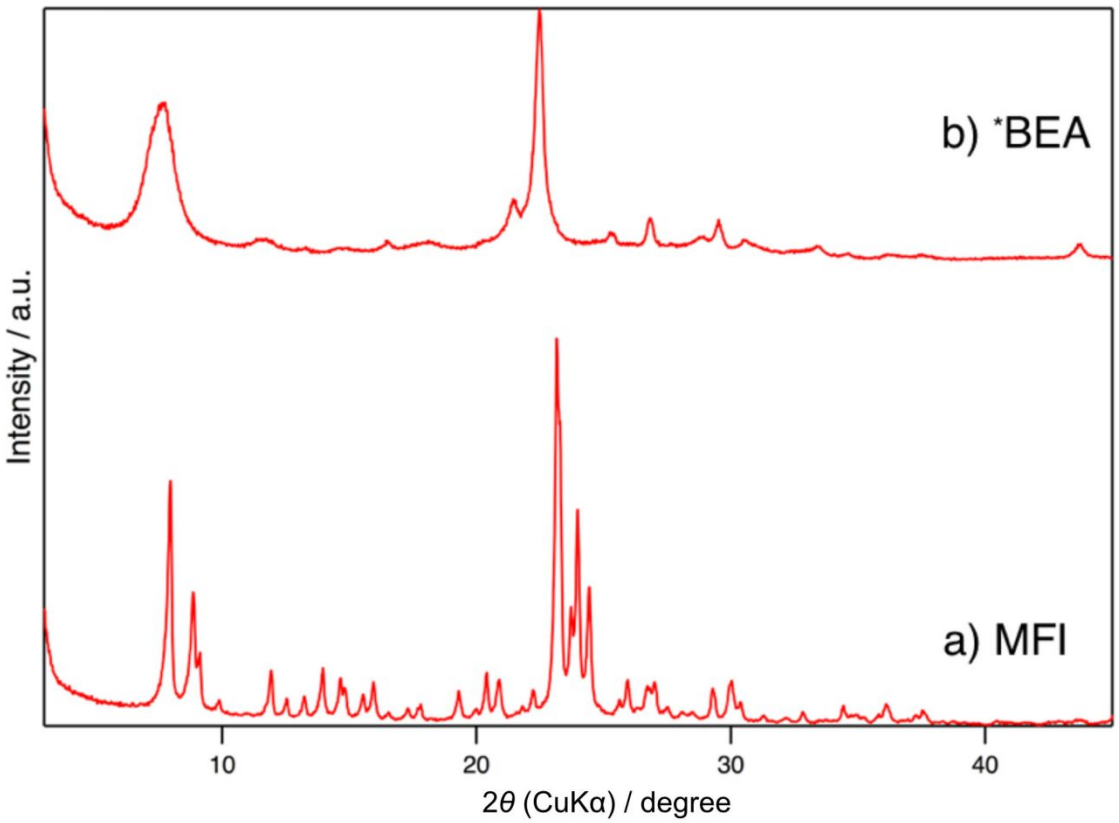

Figure S9 | CuKα XRD patterns of the MFI and *BEA zeolites: (a) MFI and (b) *BEA zeolite. Cu-Kα X-ray source was used. All the diffraction peaks are due to the corresponding zeolite structure.

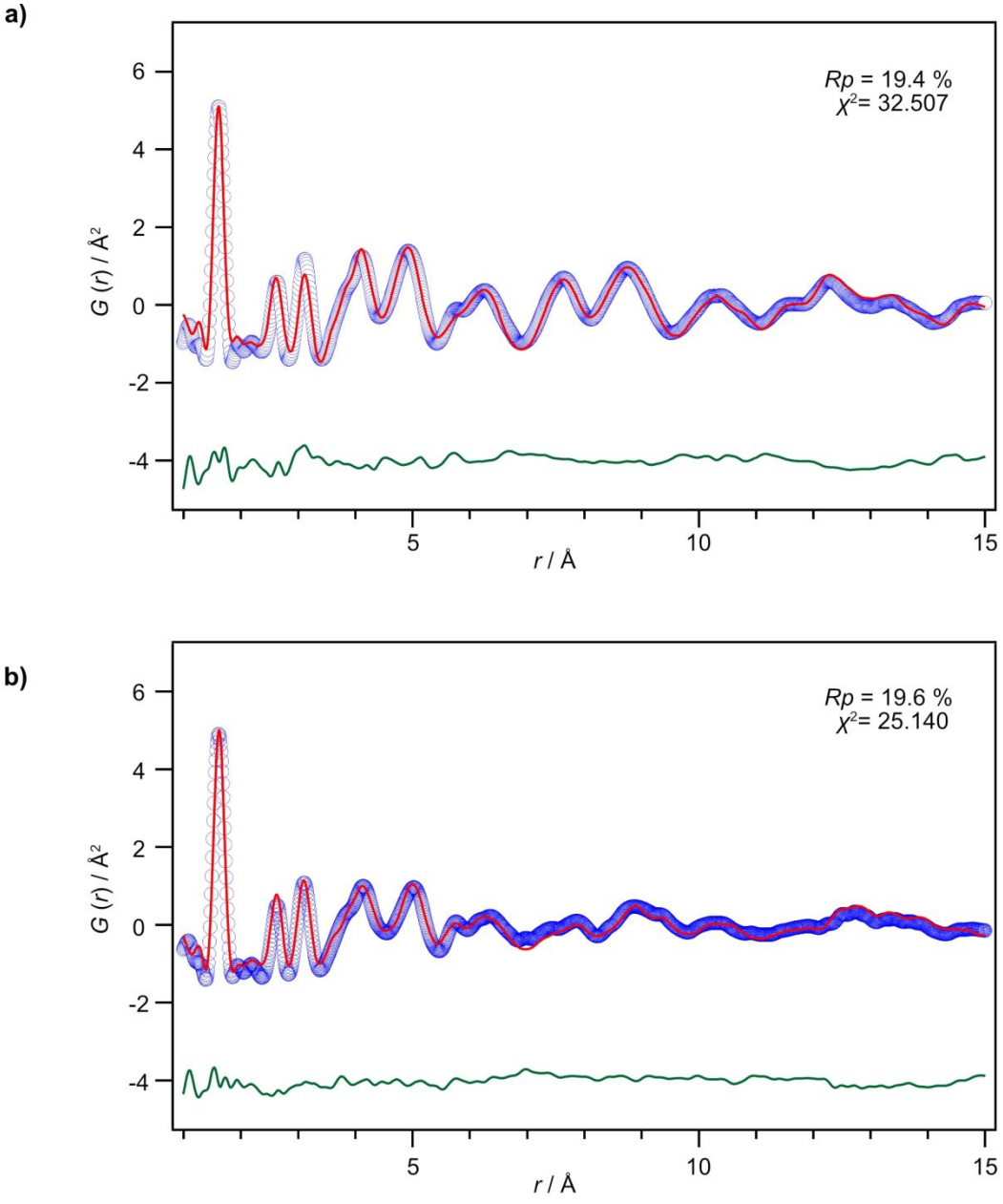

Figure S10 | Experimental and simulated PDF patterns of the MFI and *BEA zeolites: (a) MFI and (b) *BEA zeolites (red-lines correspond to the simulated patterns, the experimental data is shown in blue, and the green lines show the differences between them).

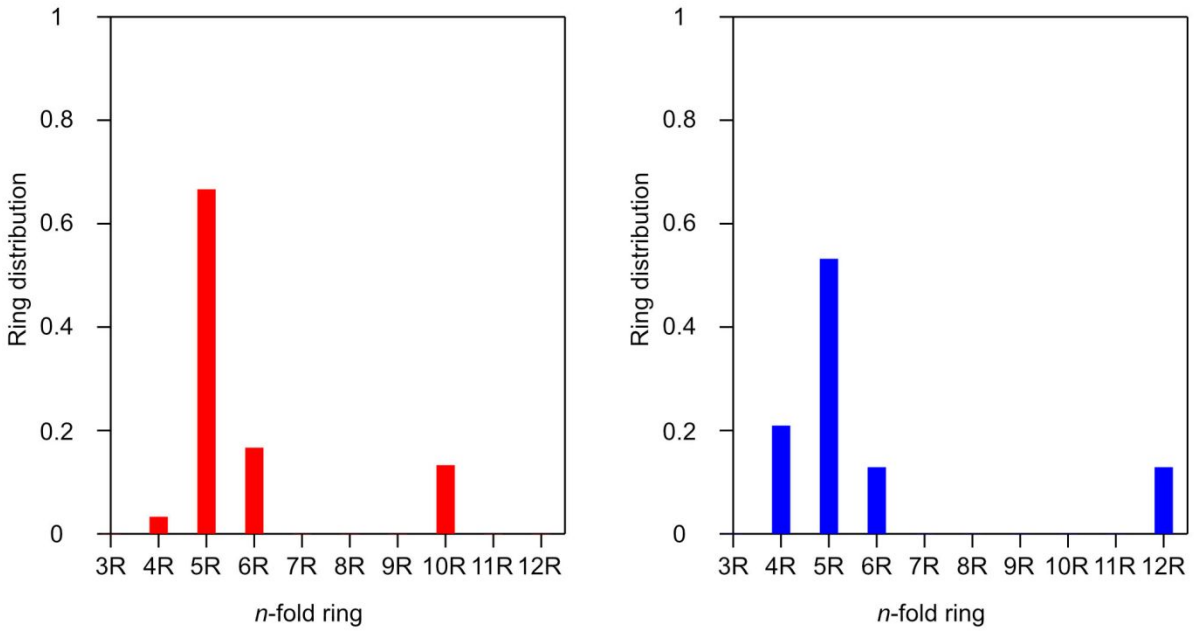

Figure S11 | Ring distribution of the MFI and *BEA zeolites: a) MFI and b) *BEA zeolites. Ring distributions are normalized for clarity.

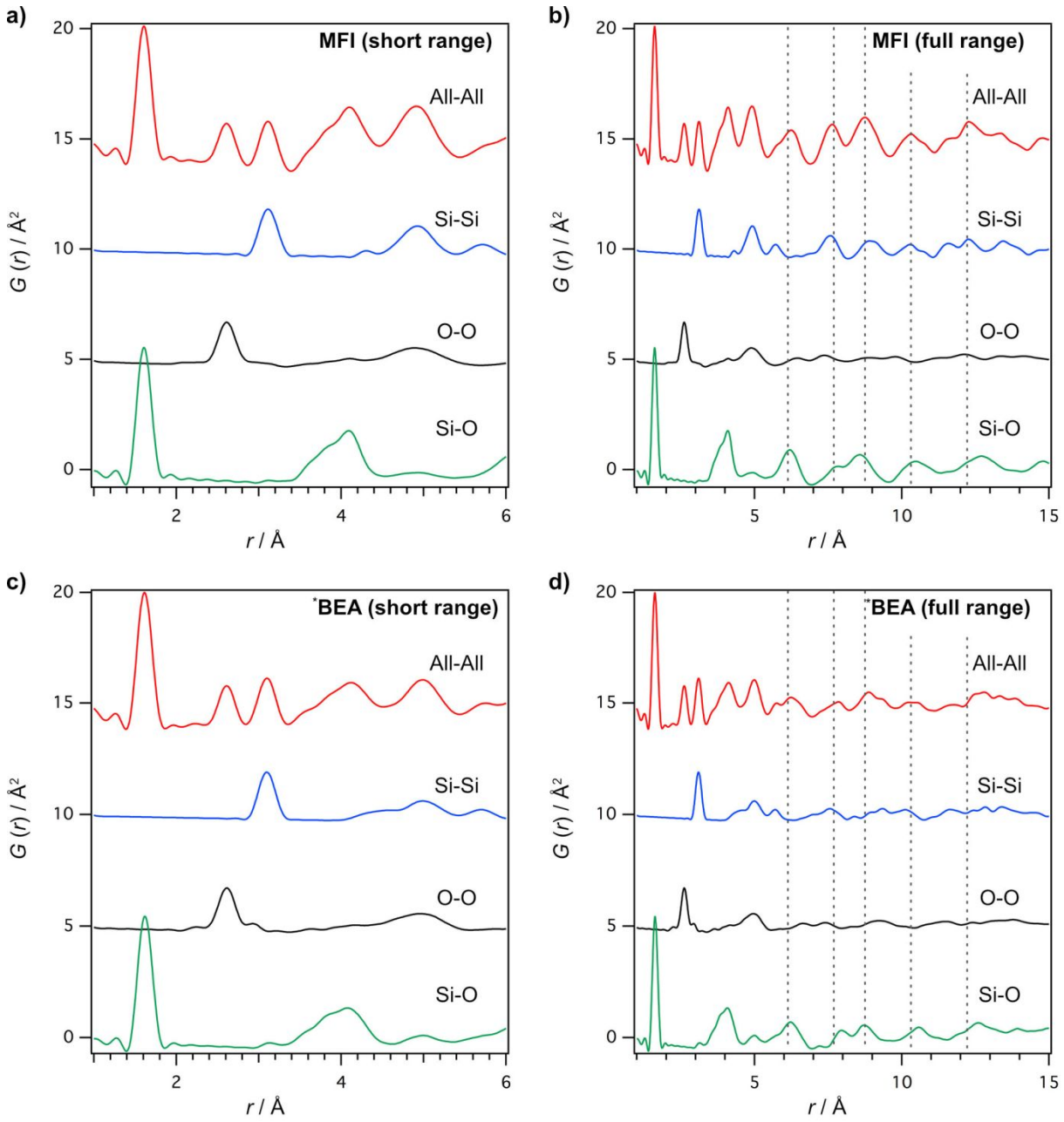

Figure S12 | Simulated patterns of partial *G* (*r*) calculated from the structural model of the MFI and *BEA zeolite: All the profiles were calculated using the PDFgui[2] software. Partial *G*(*r*) of the MFI zeolite in (a) the low *r* range (1–6 Å) and (b) the full range (1–15 Å). Partial *G*(*r*) of the *BEA zeolite in (c) the low *r* range (1–6 Å) and (d) the full range (1–15 Å). Offset value of each partial *G* (*r*) is set to 5 for clarity. The profiles indicate the probability of each pair calculated from the simulated model shown in Figure S5. Comparison of the PDF patterns of MFI with *BEA zeolites indicates the structural difference in the long range (shown as the dotted line in (b) and (d)).

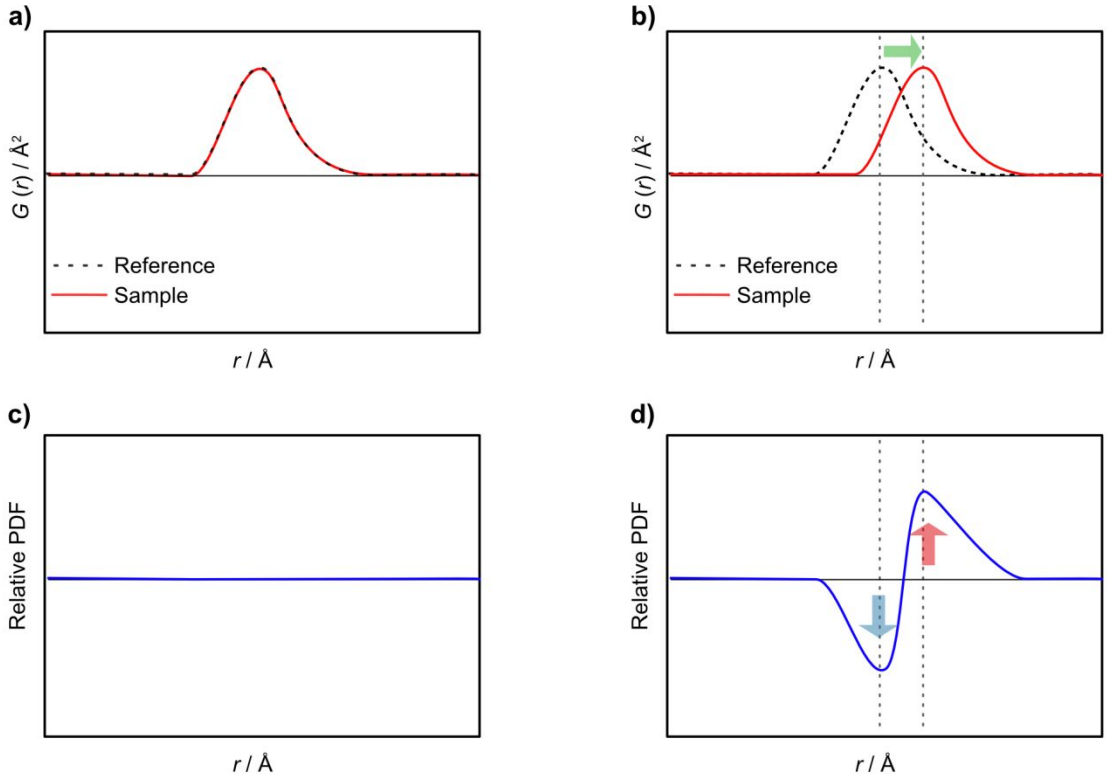

Figure S13 | Scheme of the relationship between *G*(*r*) and relative PDF patterns: (a) *G*(*r*)s of the sample and the reference with no difference; (b) *G*(*r*)s of the sample and the reference shifting the profile of the sample to the right; (c) relative PDF pattern calculated from (a); (d) relative PDF pattern calculated from (b). If there is no difference between the sample and reference profiles (a), no signal is observed in the relative PDF pattern (c). When the correlation is shifted (b), a decrease of the correlation at shorter distance and an increase at longer distance should be observed. As a result, the relative PDF pattern reflects even slight structural differences (d).

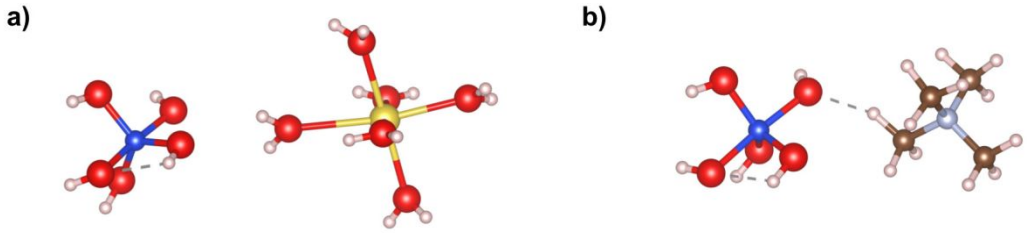

Figure S14 | Representative silicate structure containing SiO_5 species. (a) the model of the silicate species with a $Na(H_2O)_6$ cation; (b) silicate species with a tetramethylammonium cation. Quantum chemical calculations were performed to evaluate the possible presence of five-coordinated silicate species. The initial structure model was formed by assuming close contact of $Si(OH)_5$ with $Na(H_2O)_6$ or tetramethylammonium cation complex in a 15 x 15 x 15 $Å^3$. The structure was optimized by the density functional theory (DFT) using the CASTEP software with the generalized gradient approximation (GGA) and the Perdew, Burke, and Ernzerhof (PBE) exchange-correlation functional. Ultra-soft pseudopotentials and a 370-eV energy cut-off were used.

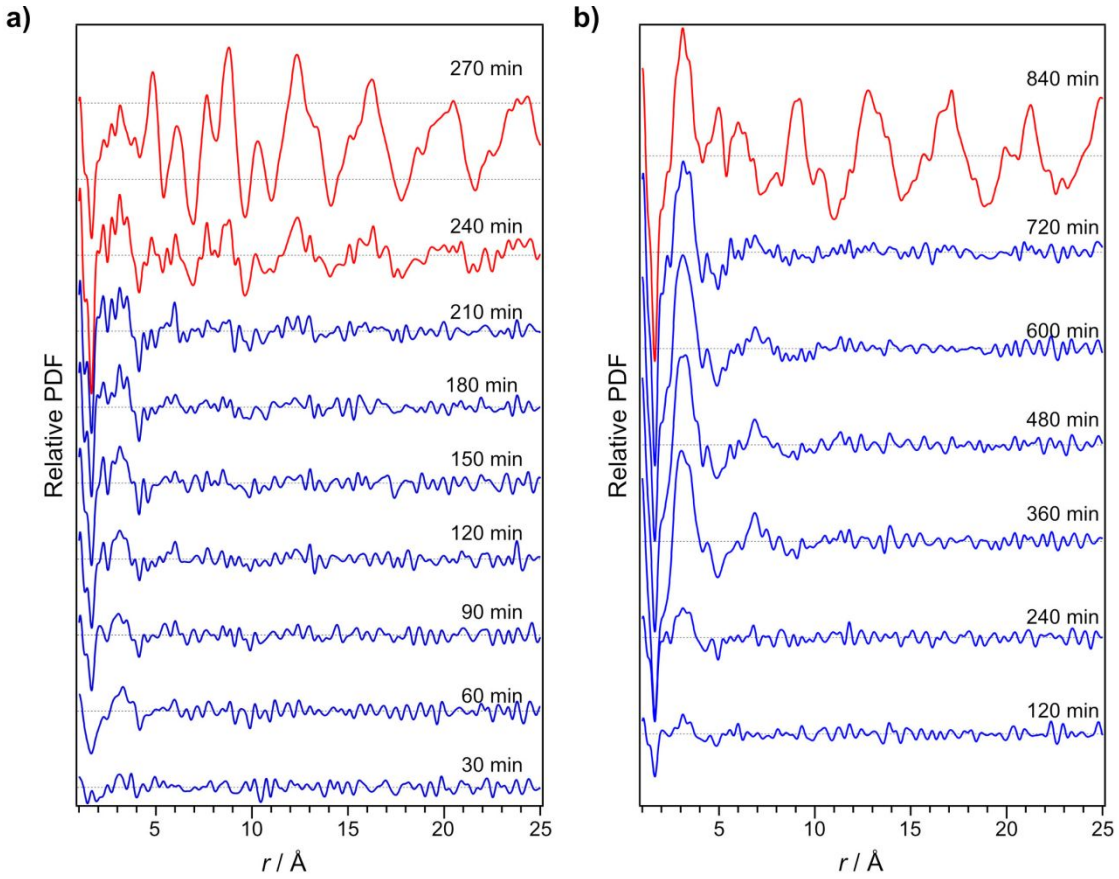

Figure S15 | *In-situ* relative PDF patterns of longer range obtained during the syntheses of MFI and *BEA zeolites. *In-situ* relative PDF patterns of (a) MFI and (b) *BEA zeolites (calculated using the scattering pattern at 0 min).

References

1. Umeda, T.; Yamada, H.; Ohara, K.; Yoshida, K.; Sasaki, Y.; Takano, M.; Inagaki, S.; Kubota, Y.; Takewaki, T.; Okubo, T.; et al. Comparative Study on the Different Interaction Pathways between Amorphous Aluminosilicate Species and Organic Structure-Directing Agents Yielding Different Zeolite Phases. *J. Phys. Chem. C* **2017**, *121* (43), 24324–24334.

2. Farrow, C. L.; Juhas, P.; Liu, J. W.; Bryndin, D.; Boin, E. S.; Bloch, J.; Proffen, T.; Billinge, S. J. L. PDFfit2 and PDFgui: Computer Programs for Studying Nanostructure in Crystals. *J. Phys. Condens. Matter* **2007**, *19* (33), 335219–335226.